

ZeroWaste Dataset: Towards Deformable Object Segmentation in Cluttered Scenes

Dina Bashkirova^{1*} Mohamed Abdelfattah² Ziliang Zhu¹ James Akl³
 Fadi Alladkani³ Ping Hu¹ Vitaly Ablavsky⁴ Berk Calli³ Sarah Adel Bargal¹
 Kate Saenko^{1,5}

¹ Boston University ²American University in Cairo ³ Worcester Polytechnic Institute
⁴ University of Washington ⁵ MIT-IBM Watson AI Lab

Abstract

Less than 35% of recyclable waste is being actually recycled in the US [2], which leads to increased soil and sea pollution and is one of the major concerns of environmental researchers as well as the common public. At the heart of the problem are the inefficiencies of the waste sorting process (separating paper, plastic, metal, glass, etc.) due to the extremely complex and cluttered nature of the waste stream. Recyclable waste detection poses a unique computer vision challenge as it requires detection of highly deformable and often translucent objects in cluttered scenes without the kind of context information usually present in human-centric datasets. This challenging computer vision task currently lacks suitable datasets or methods in the available literature. In this paper, we take a step towards computer-aided waste detection and present the first in-the-wild industrial-grade waste detection and segmentation dataset, ZeroWaste. We believe that ZeroWaste will catalyze research in object detection and semantic segmentation in extreme clutter as well as applications in the recycling domain. Our project page can be found at <http://ai.bu.edu/zerowaste/>

1. Introduction

As the world population grows and becomes increasingly urbanized, waste production is estimated to reach 2.6 billion tonnes a year in 2030, an increase from its current level of around 2.1 billion tonnes [28]. Efficient recycling

strategies are critical to reduce the devastating environmental effects of rising waste production. Materials Recovery Facilities (MRFs) are at the center of the recycling process. These facilities are where the collected recyclable waste is sorted into separate bales of plastic, paper, metal and glass (and other sub-categories). Even though the MRFs utilize a large number of machines alongside manual labor [24], the recycling rates as well as the profit margins stay at undesirably low levels (e.g. less than 35% of the recyclable waste actually got recycled in the United States in 2018 [2]). Another crucial aspect of manual waste sorting is the safety of the workers, who risk their health daily getting exposed to dangerous and unsanitary objects (e.g. knives, medical needles). At the same time, the extremely cluttered nature of the waste stream makes automated waste detection (*i.e.* detection of waste objects that should be removed from the conveyor belt) very challenging to achieve.

Recent advances in object classification and segmentation provide a great opportunity to make the recycling process more efficient, more profitable and safer for the workers. Unfortunately, the research community is lacking the high-quality in-the-wild datasets to train and evaluate the classification and segmentation algorithms for industrial waste sorting. While several companies do development in the automated waste sorting space (e.g. [49, 50, 57]), they keep their data private, and the few existing open-source datasets [38, 48, 54, 60] are very limited in the amount of data and/or are generated in uncluttered environments, not representing the complexity of the domain (see Figure 1).

In this paper, we propose the largest openly available in-the-wild waste detection dataset ZeroWaste that is specifically designed for evaluating label-efficient industrial

*dbash@bu.edu

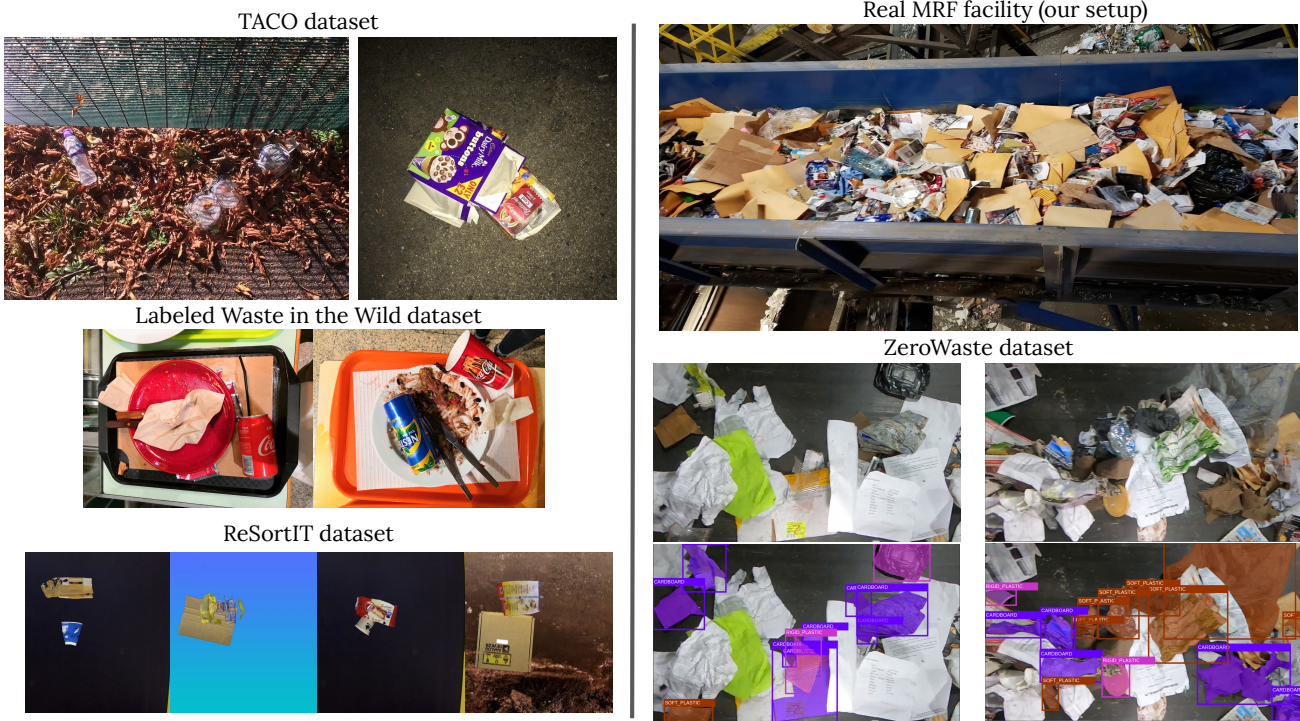


Figure 1. **Left:** examples of the existing waste detection and classification datasets (top to bottom): Trash Annotation in Context (TACO) [48], Labeled Waste in the Wild [54], ReSortIT [31] datasets. **Right:** footage of the waste sorting process at a real Materials Recovery Facilities (MRF). The domain shift between the simplified datasets with solid background and little to no clutter and the real images of the conveyor belt from the MRF, as well as the object-centric nature of the existing datasets, makes it impossible to use models trained on these datasets for automated detection on real waste processing plants. In this paper, we propose a new ZeroWaste dataset collected from a real waste sorting plant. Our dataset includes a set of densely annotated frames for training and evaluation of the detection and segmentation models, as well as a large number of unlabeled frames for semi- and self-supervised learning methods. We also include frames of the conveyor belt before and after manual collection of foreground objects to facilitate research on weakly supervised detection and segmentation. Please see Figure 2 for the illustration of our ZeroWaste dataset.

waste detection. ZeroWaste is a dataset that is fundamentally different from the popular detection and segmentation benchmarks: high level of clutter, presence of highly deformable and translucent objects, as well as a fine-grained difference between the object classes – all these aspects pose a unique challenge for the automated vision. In addition to that, due to the ever-changing nature of the stream, content and visual qualities of the stream are often MRF-specific and highly depend on the season, therefore the detection algorithm must be label-efficient and able to learn and adapt to the changes in the stream with only a few labeled examples. We envision that our open-access dataset will allow researchers to develop more robust and data-efficient algorithms for object detection and other related problems beyond human-centric domains. We summarize our contributions as follows:

1. We propose the first fully-annotated ZeroWaste- f dataset industrial waste object detection. The ZeroWaste- f dataset presents a challenging real-

life computer vision problem of detecting highly deformable objects in severely cluttered scenes. In addition to the fully annotated frames from ZeroWaste- f set, we include the unlabeled ZeroWaste- s set for semi-supervised learning. We also propose a version of our ZeroWaste data augmented with objects from the TACO [48] dataset, ZeroWasteAug, to combat class imbalance. We show that introduction of object augmentation improves the overall segmentation quality.

2. We introduce a novel before-after data collection setup and propose the ZeroWaste- w dataset for binary classification of frames before and after the collection of target objects. This binary classification setup allows much cheaper data annotation and catalyzes further development of weakly supervised segmentation and detection methods. Our experimental results show that meaningful foreground segmentation can be achieved using ZeroWaste- w , however, more efficient weakly-supervised methods are needed to reach the segmenta-

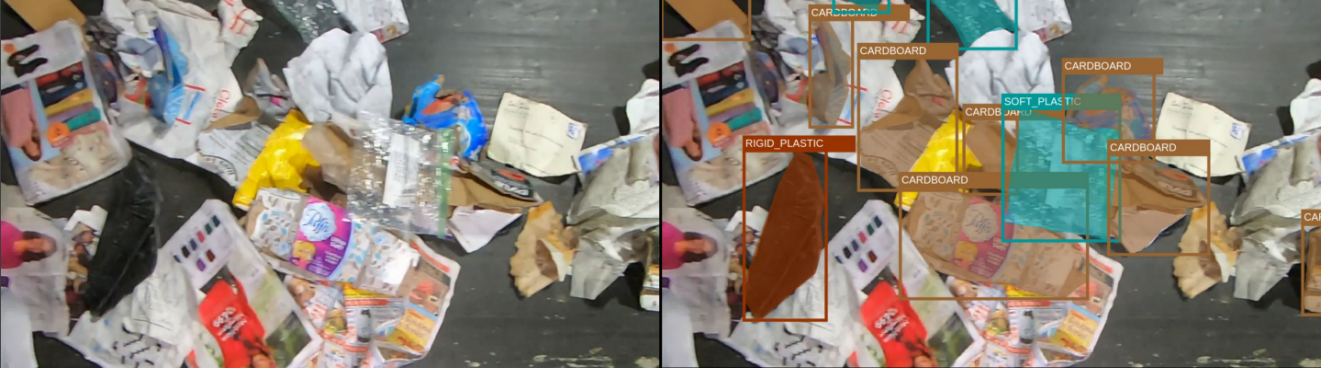


Figure 2. **Left:** example of an image from *ZeroWaste-f* dataset. **Right:** the corresponding ground truth instance segmentation. At the end of this conveyor belt, only paper objects must remain. Therefore, we annotated the removable objects of four material types as foreground: soft plastic, rigid plastic, cardboard and metal. The background includes the conveyor belt and paper objects. Severe clutter and occlusions, high variability of the foreground object shapes and textures, as well as severe deformations of objects usually not present in other segmentation datasets, make this domain very challenging for object detection. More examples of our annotated data can be found in Section 7.3 of the Appendix (*best viewed in color*).

tion quality achieved by fully-supervised methods.

3. We implement the fully-supervised detection and segmentation baselines for the *ZeroWaste-f* dataset and semi- and weakly-supervised baselines for *ZeroWaste-s* and *ZeroWaste-w* datasets. Our results show that popular detection and segmentation methods, such as Mask-RCNN, TridentNet and DeepLabV3+, struggle to generalize to our data, which indicates a challenging nature of our in-the-wild dataset and suggests that new and more robust methods must be developed to solve the problem efficiently and be applied in the real waste sorting plants.

2. Related work

Detection and Segmentation Datasets Many datasets for image segmentation have been proposed with the goal of densely recognizing general objects and “stuff” in image scenes like street view [7, 17, 61], natural scenes [9, 20, 35, 44, 65], and indoor spaces [13, 19, 53]. Yet, few of them have been designed for the more challenging vision task required in automated waste recycling. Several related datasets have been proposed that contain only image-level labels, like *Portland State University Recycling* [38] consists of labeled images of box-board, glass bottles, soda cans, crushed soda cans and plastic bottles, and a small-scale *Stanford Trash-Net* [60] dataset containing images of single waste objects from six predefined classes. Though beneficial for image-level classification in well-defined conditions, images of in these two datasets have very simple background and do not apply to waste object localization. To enable localization tasks, *Labeled Waste in the Wild* [54] annotated bounding boxes for objects of 20 waste classes. Perhaps the most similar dataset to ours is the *Trash Annotation in Context*

(*TACO*) [48] of 1500 densely annotated images containing objects of 60 litter classes. Yet *TACO* contains deliberately collected outdoor scenes with one or a few foreground objects that are rarely occluded, which makes it less practical for materials recovery scenarios (see Table 1 and Figure 1 for comparison). Another great effort towards automated waste sorting is the synthetic *ReSort-IT* [31] dataset for waste object detection on the conveyor belt, as well as the *FloW* [16] dataset of the floating waste detection in the inland waters. In contrast, our *ZeroWaste* has almost 3 times more annotated images and more than 10 times more annotated instances than *TACO* and is collected from the front lines of a waste sorting plant where the objects are frequently severely deformed and occluded, which makes our dataset the closest one to the real applications, *e.g.*, robotic grasping or waste stream analysis.

Detection and Segmentation Methods Image segmentation can be formulated as a task of classifying each pixel into a set of labels [41]. Recent semantic segmentation models [12, 37, 62, 63] have achieved state-of-the-art performance for recognizing general object/stuff classes from natural scene images. Representative frameworks like MaskRCNN [39] effectively detect objects in images and simultaneously generate high-quality masks, which enables efficient interaction between robots and target objects. Yet due to their data-hungry nature, these methods rely on large volumes of annotated data for training, which can be challenging and expensive, especially in specialized application scenarios [5]. Recycling annotation in particular requires expert labelers and is thus even more costly. Semi-supervised segmentation methods have been proposed to address such limitations by jointly learning from both annotated and

unannotated images [11, 22, 29, 40, 42, 45]. For example, ReCo [36] introduces an unsupervised loss to optimize both intra- and inter-class variance of pixels so as to further boost the segmentation performance. In a more data-efficient setting, weakly-supervised segmentation methods exploit annotations that are even easier to obtain, e.g. image-level tags [3, 30, 46]. These methods typically utilize Class Activation Maps (CAM) [64] to select the most discriminative regions, which are later used as pixel-level supervision for segmentation networks [10, 21, 56]. By constraining consistency between partial and full features, PuzzleCAM [27] effectively enhances the quality of CAMs without adding layers. All these advanced segmentation models are trained on large-scale general-purpose data, such as MS-COCO [35] or PASCAL VOC [20], and applying them to the cluttered real-world scenarios presents challenges like domain shift and poor generalization. We provide the experimental results on the popular fully-, semi- and weakly-supervised semantic segmentation and object detection methods on our ZeroWaste dataset and analyze their performance on this real industrial task.

3. ZeroWaste Dataset

In this section, we describe our ZeroWaste-*f* dataset for fully supervised detection and evaluation, unlabeled ZeroWaste-*s* for semi-supervised learning, ZeroWaste-*w* of images before and after the removal of target objects for weakly supervised detection, and ZeroWasteAug of multi-domain augmented waste objects for comparison in all fully-, semi-, and weakly-supervised settings. The datasets are licensed under the Creative Commons Attribution-NonCommercial 4.0 International License [1]. The MRF at which the data was collected agreed to release the data for any non-commercial purposes and decided to remain unacknowledged.

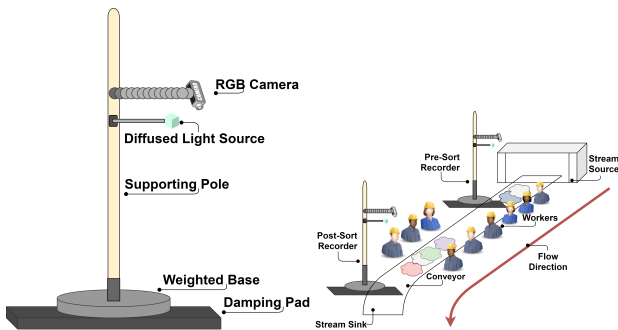


Figure 3. The footage recording setup is designed to fit the constraints of the facility environment. **Left:** Assembly of each recording apparatus. **Right:** Layout of the recording setup in the recycling environment.

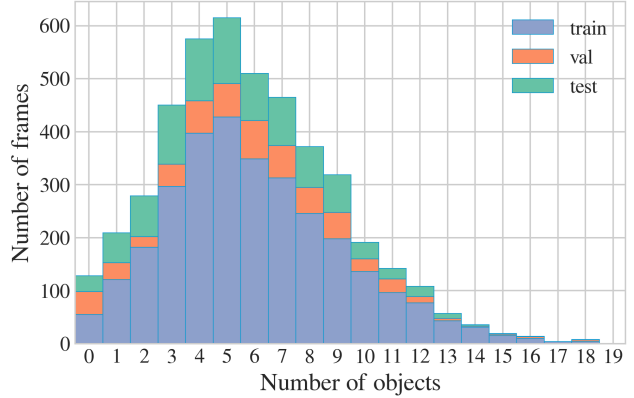


Figure 4. Statistics of the number of *foreground* objects per frame in train, val and test splits of ZeroWaste-*f*. The overall number of objects in the scene, including paper objects, is much higher (*best viewed in color*).

Data Collection and Pre-processing The data was collected from a high-quality paper conveyor of a single stream recycling facility in Massachusetts. The sorting operation on this conveyor aims to keep high quality paper and consider anything else as contaminants including non-paper items (*e.g.* metal, plastic, brown paper, cardboard, boxboard). We collected data during the regular operation of the MRF using two compact recording installations at the start and end of the conveyor belt (see Fig. 6), that is, footage is captured simultaneously both at the unsorted and sorted sections of the same conveyor. The recording apparatus is designed to fit the constraints of the facility: In order not to disrupt the MRF operation and be able to work in confined spaces available near the conveyor the recording platform needs to be compact, non-intrusive (to the workers), and portable (easy to move, battery-powered). Note that the cameras are not directly mounted on the conveyor but to a stand-alone platform, to reduce vibrations transmitted to the cameras. Additional considerations are made (see Figure 3): (1) Damping pads are installed to counter the ground vibrations of the heavy machinery and reduce vibrations on the camera even further; (2) Weighted bases lower the center of mass to keep the apparatus stable. We used the GoPro Hero 7 camera to collect the video data, and installed two LitraTorch 2.0 portable lamps with a light diffuser to maintain consistent lighting. Both cameras were installed at around 100 cm above the conveyor, and the light sources at around 80 cm.

Sequences of 12 videos of total length of 95 minutes and 14 seconds with FPS 120 and size 1920×1080 were collected and processed through the following steps:

1. Rotation and cropping. The frames were rotated so that the conveyor belt is parallel to the frame borders and cropped to remove the regions outside the conveyor belt.

We ensured that any personal information or identifiable footage of the workers at the conveyor belt was excluded from our data.

2. Optical distortion. We removed the distortion [8] using the OpenCV [6] library to compensate for the fish-eye effect caused by the proximity of the cameras to the conveyor belt.
3. Deblurring. We used the SRN-Deblur [55] method to remove motion blur resulting from the fast-moving conveyor belt. According to our visual inspection, SRN-Deblur achieves satisfactory deblurring and does not introduce the undesired artifacts that usually appear when classical deconvolution-based methods are used.

The illustration of the original frames shot at the beginning of the conveyor belt and the corresponding preprocessing results can be found in Figure 12 in Section 7.3 of the Appendix.

Densely Annotated ZeroWaste-*f* and Unlabeled ZeroWaste-*s* Datasets The fully annotated ZeroWaste-*f* dataset consists of 4661 frames sampled from the processed videos and the corresponding ground truth polygon segmentation. We used the open-source CVAT [51] annotation toolkit to manually collect the polygon annotations of objects of four material types: cardboard, soft plastic, rigid plastic and metal. We chose this set of class labels following the MRF’s guidelines for the workers to collect cardboard, plastic and metal into separate bins, as well as the fact that grasping of rigid and non-rigid objects might require the use of fundamentally different kinds of robotic systems. We annotated 1805 frames with a subsampling rate of 10 to enable training and evaluation of object tracking methods, as well as 2616 frames with a subsampling rate of 100 to increase the dataset diversity. The polygon annotation was performed according to the following set of rules:

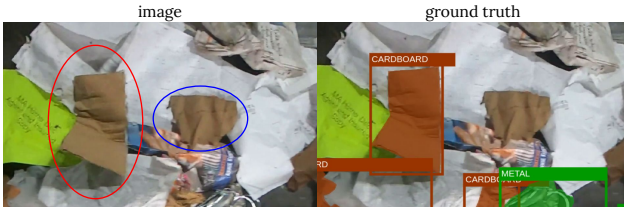


Figure 5. **Left:** example of an image from ZeroWaste-*f* dataset. **Right:** the corresponding ground truth instance segmentation. Expert training and common sense knowledge are required to distinguish between the cardboard object on the left (red circle) and the brown paper on the right (blue circle), as they are visually very similar but differ in thickness and rigidity. Trained annotators achieve average pixel-level precision of 79.57% and recall of 71.96% for the cardboard class. (*best viewed in color*).



Figure 6. We installed two stationary cameras above the conveyor belt: one at the beginning of the line and another one at the end. At this particular conveyor belt, workers are asked to remove objects of any material other than paper, such as cardboard, plastic and metal. Therefore, the footage collected from the beginning of the line contains the “foreground” objects that need to be removed, and the frames from the end of the conveyor belt are supposed to only contain the “background” paper objects. We used this setup as a foundation of our ZeroWaste-*w* dataset.

1. Objects of four material types were annotated as foreground: cardboard (including parcel packages, boxboard such as cereal boxes and other carton food packaging), soft plastic (*e.g.* plastic bags, wraps), rigid plastic (*e.g.* food containers, plastic bottles) and metal (*e.g.* metal cans). Paper objects were treated as background.
2. A polygon must include all foreground object pixels, and it might include a small amount of background pixels.
3. If an object is partially occluded and separate parts are visible, we annotated them as separate objects, since it is impossible to certainly tell whether it is one or several visually similar objects.

Each annotated video frame was validated by an independent reviewer to pass the standards above (see Figure 2). The review process was performed by the students and researchers with a computer science background specifically trained to perform the annotation. We did not delegate the annotation to the crowd-sourcing platforms, such as Amazon Mechanical Turk [18], due to the complexity of the domain that requires expert knowledge to be able to detect and correctly classify the foreground objects (see the illustration in Figure 5). Instead, the professional annotators have been hired via Upwork¹ to annotate the frames, with the

¹<https://www.upwork.com/>

Split	#Images	Cardboard	Soft Plastic	Rigid Plastic	Metal	#Objects	Domain
Train	3002	12940	4862	1160 +2778	263 +4373	19225 +7151	Real
Validation	572	2167	855	305 +637	60 +1010	3387 +1647	
Test	929	3428	1236	315 +886	63 +990	5042 +1876	
Unlabeled	6212	-	-	-	-	-	
Total	10715	18535	6953	1780 +4301	386 +6370	27744 +10584	
TACO	1499	240	652	1183	506	2581	Real
ReSortIT	16000	8000	8000	8000	8000	32000	Synthetic

Table 1. Statistics of the total number of objects in the training, validation and test splits of ZeroWasteAug and ZeroWaste-*f* datasets, in comparison with TACO [48] dataset with labels mapped to our set of classes and the Synthetic Complex subset of the ReSortIT [31] dataset. The numbers written in green, e.g. +10584, reflect the number of augmented objects added in ZeroWasteAug. Row 4 presents the unlabeled ZeroWaste-*s* set of images for semi-supervised learning.

estimated average time spent on the annotation and review about 12.5 minutes per frame (details on that can be found in Section 7.4 of Appendix). Each frame was assessed by an expert reviewer for consistency and quality control. The resulting average annotation agreement across 20 frames is 84.2% before expert review and above 94% after the review, more details on the human annotation agreement can be found on Figure 7. The dataset was split into training, validation and test splits and stored in the widely used MS COCO [35] format for object detection and segmentation using the open-source Voxel51 toolkit [43]. Please refer to Table 1 and Figure 4 for more details about the class-wise statistics of all splits. In addition, we provide 6212 unlabeled images that comprise ZeroWaste-*s* dataset. ZeroWaste-*s* can be used to refine the detection using semi-supervised or self-supervised learning methods.

ZeroWasteAug Dataset As seen in Table 1, there is a significant imbalance in the class distribution of the collected ZeroWaste dataset that can degrade the performance of the detection methods, e.g. metal objects are more than 40 times more rare than the cardboard. ZeroWasteAug comprises a version of ZeroWaste-*f* in which frames were augmented with the objects of the rare metal and rigid plastic classes that were cropped out of TACO [48] dataset. To minimize the domain shift between the TACO objects and the ZeroWaste frames, the contrast, brightness, and blurriness of each cropped object were changed to match the average value of the frame on which the object was augmented. Random resizing, cropping, mirroring were applied on each TACO object before augmentation (please refer to Figure 15 for the examples).

Weakly supervised ZeroWaste-*w* Dataset We leverage the videos taken of the conveyor belt before and after the removal of the foreground objects to create a weakly-supervised ZeroWaste-*w* dataset. This dataset contains 1202 frames with the foreground objects (*before* class) and 1208 frames without the foreground objects (*after* class).

	AP	AP50	AP75	APs	APm	APl
RetinaNet	21.0	33.5	22.2	4.3	9.5	22.7
MaskRCNN	22.8	34.9	24.4	4.6	10.6	25.8
TridentNet	24.2	36.3	26.6	4.8	10.7	26.1

Table 2. Mean average precision on the test set of ZeroWaste-*f* of MS-COCO-pretrained Mask R-CNN, TridentNet and RetinaNet finetuned on ZeroWaste-*f*. Please refer to Table 4 and Figure 8 in the Appendix for class-wise results.

One advantage of such a setup is that it is relatively cheap to acquire the ground truth labels (only an image-level inspection is required to ensure there are no false negatives in the *after* class subset). The ZeroWaste-*w* dataset is specifically collected to be used in the weakly-supervised setup and is meant to provide an alternative and more data-efficient solution to the problem. The ground truth instance segmentation is available for all images of the *before* class as it overlaps with the ZeroWaste-*f* dataset. Please see Figure 6 for examples of ZeroWaste-*w* dataset.

4. Experiments

In this section, we provide baseline results for our proposed ZeroWaste dataset. We perform fully-supervised object detection on ZeroWaste-*f* using the most widely used Mask R-CNN [39], RetinaNet [34], TridentNet [33] models, and we train DeepLabV3+ [14] as a semantic segmentation baseline. We also perform fully- and semi-supervised semantic segmentation on ZeroWaste-*s* using the ReCo [36] and CCT [45], and report the weakly-supervised segmentation results of RISE [47] CAMs, PuzzleCAM [27] and EPS [32] trained on ZeroWaste-*w*. We will provide the implementation and a detailed description of our experiments in the supplementary material.

Method	Supervision	Validation		Test	
		mIoU	Pixel Acc.	mIoU	Pixel Acc.
Trained with ZeroWaste- <i>w</i>					
<i>Random</i>	none	7.2	75.3	8.4	71.8
<i>CAM</i>	<i>weak-w</i>	16.7	31.4	19.1	33.7
<i>PuzzleCAM</i>	<i>weak-w</i>	29.87	67.63	28.46	65.96
<i>EPS</i>	<i>weak-w</i>	34.56	57.98	34.06	57.20
Trained with ZeroWaste- <i>f</i> and ZeroWaste- <i>s</i>					
<i>DeepLabv3+</i>	<i>full</i>	46.93	90.62	52.13	91.38
<i>DeepLabv3+</i>	<i>full+aug</i>	47.48	90.69	52.50	91.44
<i>ReCo</i>	<i>full</i>	51.30	89.22	52.28	89.33
<i>ReCo</i>	<i>semi</i>	49.49	89.58	44.12	88.36
<i>CCT</i>	<i>full</i>	30.79	84.80	29.32	85.91
<i>CCT</i>	<i>semi</i>	28.70	86.33	32.49	87.30
<i>EPS</i>	<i>weak-f</i>	13.75	59.96	13.91	60.65

Table 3. Results on validation and test sets of the ZeroWaste-*f* dataset of fully-, semi-, and weakly- supervised learning methods, separately trained on original non-augmented datasets and the augmented ZeroWasteAug dataset. ‘*weak-w*’, ‘*weak-f*’, and ‘*weak-aug*’ denote weak image-level supervision from ZeroWaste-*w* (before/after labels), ZeroWaste-*f* (class-wise labels), and ZeroWasteAug (class-wise labels) respectively. More details can be found in section 7.2 of Appendix.

4.1. Object Detection

Experiments It has been shown that pretraining the model on a large-scale dataset, such as MS COCO [35], improves generalization and helps to prevent overfitting [23, 26, 52]. Therefore, in our first experiments, we used the model with weights learned on COCO and further fine-tuned it with our ZeroWaste-*f* dataset. We used a standard implementation of the popular Mask R-CNN, RetinaNet [34] and the TridentNet [33] models both with ResNet-50 [25] backbone. We used the Detectron2 [58] library in all of the experiments. The model was finetuned for 40000 iterations on the training set of our ZeroWaste-*f* dataset on a single Geforce GTX 1080 GPU with batch size 8. To compensate for a relatively small number examples in the training set and to avoid overfitting, we leveraged heavy data augmentation, including random rotation and cropping, adjustment of brightness and hue, *etc.* We report the experimental results in Table 2 (COCO → ZeroWaste section). A more detailed description of the results can be found in Section 7.1 of Appendix.

Results and Analysis The experimental results of Mask R-CNN, TridentNet and RetinaNet indicate that the proposed ZeroWaste dataset is significantly challenging for the state-of-the-art detection methods, with TridentNet performing slightly better than other methods. All methods especially struggle with small objects, which are usually

harder to label correctly. Additional results of the models pretrained on TACO dataset with labels mapped to ZeroWaste set of labels show that finetuning from a TACO-pretrained model slightly improves the detection precision (see Table 4 in the Appendix). Recalling the history of success with other complex segmentation and detection datasets (*e.g.* from mIoU 57% in 2015 [4] to 84% in 2020 [15] on CityScapes [17], or from AP50 29.9 [35] in 2015 to 61.3 [59] on MS-COCO [35] in 2021, and knowing that the task *can* be solved by humans with a little training, we believe that the computer vision community will eventually come up with efficient methods for this challenging task.

4.2. Semantic Segmentation

Fully-supervised Experiments We used the state-of-the-art DeepLabv3+ [14] model as a fully-supervised semantic segmentation baseline for our dataset. DeepLabv3+ combines the atrous convolutions to extract features in multiple scales with an encoder-decoder paradigm to gradually sharpen the object boundary using the intermediate features. We used the model with ResNet-101 backbone with three 3×3 convolutions, froze the first three stages of the backbone, and separately fine-tuned the model on the training sets of ZeroWaste-*f* and ZeroWasteAug.

Semi-supervised Experiments For a semi-supervised segmentation baseline, we used the official implementation of Regional Contrast [36] (ReCo) and CCT [45] methods. ReCo utilizes the pixel-level local context and the global context represented in the semantic class relationships across the entire dataset, and the conventional Mean Teacher Framework in which a teacher network is used to generate pseudo-labels for the unlabeled images. CCT uses cross-consistency training that forces the predicted segmentation masks of unlabeled examples produced by decoders with various types of augmentations to be consistent. For comparison, we conducted four experiments with ReCo and CCT on ZeroWaste-*s* in both the fully-supervised and semi-supervised learning settings. We used the default hyperparameters for both methods.

Weakly-supervised Experiments For weakly-supervised segmentation, we followed the standard procedure based on generating Class Activation Maps (CAMs) to serve as pseudo-labels for training a segmentation network. To do so, we conducted three experiments in which we trained a classifier using image-level labels from 1) ZeroWaste-*w* (before/after labels) and 2) ZeroWaste-*f* (multiclass labels). For CAM generation, we incorporated the current state-of-the-art PuzzleCam [27] and EPS [32] methods that enhances CAM object coverage by matching the CAM of an entire image with those produced for the non-overlapping tiles of the



Figure 7. **Left:** Semantic segmentation confusion matrix of the manual annotations over 20 frames represents human expert agreement after expert review, with the average pixel-level agreement above 94% (see Figure 16 of the Supplementary for the corresponding confusion matrix *before* expert review). **Center:** Confusion matrix of DeepLabV3+ on the test split of ZeroWaste- f . **Right:** Confusion matrix of DeepLabV3+ on the test split of ZeroWaste- f when trained on ZeroWasteAug.

image. We then threshold the generated CAMs with 0.45 to produce pseudo segmentation labels for training the DeepLabv3+ segmentation network.

Results and Analysis Experimental results for fully-, semi- and weakly- supervised experiments are presented in Table 3. Class-wise results and visualizations can be found in Section 7.2 of the Appendix. Table 3 results indicate that our in-the-wild ZeroWaste dataset proposes a challenging semantic segmentation task. The confusion matrices on Figure 7 (center) show that the fully-supervised DeepLabV3+ can distinguish cardboard from paper in only 58% of the cases, and misclassifies most rigid plastic objects as soft plastic. Additionally, metal objects are often segmented as background as they appear rarely in the original dataset. Further, training on ZeroWasteAug substantially improves the pixel accuracy of the rare metal class on the original non-augmented test split of ZeroWaste- f (see Figure 7, right), but reduces the performance on the rigid plastic. This suggests that instance-level data augmentation can be an efficient technique for semantic segmentation that reduces the generalization gap on the class-imbalanced data. The semi-supervised learning results indicate that the unlabeled examples from the ZeroWaste- s subset significantly worsened the performance of ReCo. This suggests that, while the inductive bias of the ReCo model that efficiently utilizes the object context information (*i.e.* surrounding background pixels) is not efficient for ZeroWaste that has little to no context prior. In contrast, CCT performance increases slightly when the unlabeled examples are added during training, which suggests that the contrastive approach is more efficient for the proposed dataset. Additionally, results of the weakly-supervised experiments show that a simple CAM-based approach, as well as the state-of-the-art weakly supervised PuzzleCAM with cheap image-level annotations provide meaningful object localization cues.

5. Impact and Limitations of ZeroWaste

Societal Impact We believe that human-robot collaboration is essential for more efficient computer-aided recycling, quality control of the sorting process, as well as in establishing safer work conditions for the MRF workers, *e.g.* by detecting dangerous waste items. In the big picture, establishing a human-robot workflow that can maximize efficiency, profit, safety and work quality in MRFs is an essential need to address the critical waste problem in an equitable and just manner.

Limitations and Future Directions Despite the fact that ZeroWaste is the largest public dataset for waste detection to date, it is still smaller than the standard large-scale benchmarks due to the fact that the annotation process for this domain is very expensive. As future work, we plan to increase the dataset diversity by using synthetic-to-real domain adaptation and other data augmentation techniques. **Acknowledgements** This paper was supported in part by the National Science Foundation under grant FW-HTF-RL #1928506.

6. Conclusion

This work introduces ZeroWaste, which is the largest public dataset for waste detection up to date. ZeroWaste is designed as a benchmark for the training and evaluation of fully, weakly, and semi-supervised detection and segmentation methods, and can be used for various other tasks including label-efficient learning. We provide baseline results for the most popular fully, weakly, semi-supervised, and transfer learning techniques. Our results show that current state-of-the-art detection and segmentation methods cannot efficiently handle this complex in-the-wild domain. We anticipate that our dataset will motivate the computer vision community to develop more data-efficient methods applicable to a wider range of real-world computer vision problems.

References

- [1] Creative commons attribution-noncommercial 4.0 international license. [EB/OL]. <http://creativecommons.org/licenses/by-nc/4.0/> Accessed May 22, 2021. 4
- [2] United States Environmental Protection Agency. National overview: Facts and figures on materials, wastes and recycling. [EB/OL]. 1
- [3] Jiwoon Ahn and Suha Kwak. Learning pixel-level semantic affinity with image-level supervision for weakly supervised semantic segmentation. In *CVPR*, 2018. 4
- [4] Vijay Badrinarayanan, Alex Kendall, and Roberto Cipolla. Segnet: A deep convolutional encoder-decoder architecture for image segmentation. *IEEE transactions on pattern analysis and machine intelligence*, 39(12):2481–2495, 2017. 7
- [5] Adela Barriuso and Antonio Torralba. Notes on image annotation. *arXiv preprint arXiv:1210.3448*, 2012. 3
- [6] G. Bradski. The OpenCV Library. *Dr. Dobbs's Journal of Software Tools*, 2000. 5
- [7] Gabriel J Brostow, Jamie Shotton, Julien Fauqueur, and Roberto Cipolla. Segmentation and recognition using structure from motion point clouds. In *ECCV*, 2008. 3
- [8] Duane C Brown. Decentering distortion of lenses. *Photogrammetric Engineering*, 1966. 5
- [9] Holger Caesar, Jasper Uijlings, and Vittorio Ferrari. Coco-stuff: Thing and stuff classes in context. In *CVPR*, 2018. 3
- [10] Yu-Ting Chang, Qiaosong Wang, Wei-Chih Hung, Robinson Piramuthu, Yi-Hsuan Tsai, and Ming-Hsuan Yang. Weakly-supervised semantic segmentation via sub-category exploration. In *CVPR*, 2020. 4
- [11] Liang-Chieh Chen, Raphael Gontijo Lopes, Bowen Cheng, Maxwell D Collins, Ekin D Cubuk, Barret Zoph, Hartwig Adam, and Jonathon Shlens. Semi-supervised learning in video sequences for urban scene segmentation. *ECCV*, 2020. 4
- [12] Liang-Chieh Chen, George Papandreou, Florian Schroff, and Hartwig Adam. Rethinking atrous convolution for semantic image segmentation. *arXiv preprint arXiv:1706.05587*, 2017. 3
- [13] Liang-Chieh Chen, Yukun Zhu, George Papandreou, Florian Schroff, and Hartwig Adam. Encoder-decoder with atrous separable convolution for semantic image segmentation. In *ECCV*, 2018. 3
- [14] Liang-Chieh Chen, Yukun Zhu, George Papandreou, Florian Schroff, and Hartwig Adam. Encoder-decoder with atrous separable convolution for semantic image segmentation. In *ECCV*, 2018. 6, 7, 12, 13
- [15] Bowen Cheng, Maxwell D Collins, Yukun Zhu, Ting Liu, Thomas S Huang, Hartwig Adam, and Liang-Chieh Chen. Panoptic-deeplab: A simple, strong, and fast baseline for bottom-up panoptic segmentation. In *Proceedings of the IEEE/CVF Conference on Computer Vision and Pattern Recognition*, pages 12475–12485, 2020. 7
- [16] Yuwei Cheng, Jiannan Zhu, Mengxin Jiang, Jie Fu, Changsong Pang, Peidong Wang, Kris Sankaran, Olawale Onabola, Yimin Liu, Dianbo Liu, et al. Flow: A dataset and benchmark for floating waste detection in inland waters. In *Proceedings of the IEEE/CVF International Conference on Computer Vision*, pages 10953–10962, 2021. 3
- [17] Marius Cordts, Mohamed Omran, Sebastian Ramos, Timo Rehfeld, Markus Enzweiler, Rodrigo Benenson, Uwe Franke, Stefan Roth, and Bernt Schiele. The cityscapes dataset for semantic urban scene understanding. In *CVPR*, 2016. 3, 7
- [18] Kevin Crowston. Amazon mechanical turk: A research tool for organizations and information systems scholars. In *Shaping the future of ict research. methods and approaches*, pages 210–221. Springer, 2012. 5
- [19] Angela Dai, Angel X Chang, Manolis Savva, Maciej Halber, Thomas Funkhouser, and Matthias Nießner. Scannet: Richly-annotated 3d reconstructions of indoor scenes. In *CVPR*, 2017. 3
- [20] M. Everingham, L. Van Gool, C. K. I. Williams, J. Winn, and A. Zisserman. The pascal visual object classes (voc) challenge. *IJCV*, 88:303–338, 2010. 3, 4
- [21] Junsong Fan, Zhaoxiang Zhang, Chunfeng Song, and Tieniu Tan. Learning integral objects with intra-class discriminator for weakly-supervised semantic segmentation. In *CVPR*, 2020. 4
- [22] Geoff French, Timo Aila, Samuli Laine, Michal Mackiewicz, and Graham Finlayson. Semi-supervised semantic segmentation needs strong, high-dimensional perturbations. *arXiv preprint arXiv:1906.01916*, 2019. 4
- [23] Ross Girshick, Jeff Donahue, Trevor Darrell, and Jitendra Malik. Rich feature hierarchies for accurate object detection and semantic segmentation. In *Proceedings of the IEEE conference on computer vision and pattern recognition*, pages 580–587, 2014. 7
- [24] Sathish Paulraj Gundupalli, Subrata Hait, and Atul Thakur. A review on automated sorting of source-separated municipal solid waste for recycling. *Waste management*, 60:56–74, 2017. 1
- [25] Kaiming He, Xiangyu Zhang, Shaoqing Ren, and Jian Sun. Deep residual learning for image recognition. In *Proceedings of the IEEE conference on computer vision and pattern recognition*, pages 770–778, 2016. 7
- [26] Minyoung Huh, Pulkit Agrawal, and Alexei A Efros. What makes imagenet good for transfer learning? *arXiv preprint arXiv:1608.08614*, 2016. 7
- [27] Sanghyun Jo and In-Jae Yu. Puzzle-cam: Improved localization via matching partial and full features. *CVPR*, 2021. 4, 6, 7, 12
- [28] Silpa "Kaza, Lisa C. Yao, Perinaz Bhada-Tata, and Frank Van Woerden. "What a Waste 2.0 : A Global Snapshot of Solid Waste Management to 2050". "World Bank", "Washington, DC", "2018". 1
- [29] Jongmok Kim, Jooyoung Jang, and Hyunwoo Park. Structured consistency loss for semi-supervised semantic segmentation. *arXiv preprint arXiv:2001.04647*, 2020. 4
- [30] Alexander Kolesnikov and Christoph H Lampert. Seed, expand and constrain: Three principles for weakly-supervised image segmentation. In *ECCV*, 2016. 4

- [31] Maria Koskinopoulou, Fredy Raptopoulos, George Papadopoulos, Nikitas Mavrakis, and Michail Maniadas. Robotic waste sorting technology: Toward a vision-based categorization system for the industrial robotic separation of recyclable waste. *IEEE Robotics & Automation Magazine*, 28(2):50–60, 2021. 2, 3, 6
- [32] Seungho Lee, Minhyun Lee, Jongwuk Lee, and Hyunjung Shim. Railroad is not a train: Saliency as pseudo-pixel supervision for weakly supervised semantic segmentation. In *Proceedings of the IEEE/CVF Conference on Computer Vision and Pattern Recognition*, pages 5495–5505, 2021. 6, 7
- [33] Yanghao Li, Yuntao Chen, Naiyan Wang, and Zhaoxiang Zhang. Scale-aware trident networks for object detection. In *Proceedings of the IEEE/CVF International Conference on Computer Vision*, pages 6054–6063, 2019. 6, 7
- [34] Tsung-Yi Lin, Priya Goyal, Ross Girshick, Kaiming He, and Piotr Dollár. Focal loss for dense object detection. In *Proceedings of the IEEE international conference on computer vision*, pages 2980–2988, 2017. 6, 7
- [35] Tsung-Yi Lin, Michael Maire, Serge Belongie, James Hays, Pietro Perona, Deva Ramanan, Piotr Dollár, and C Lawrence Zitnick. Microsoft coco: Common objects in context. In *European conference on computer vision*, pages 740–755. Springer, 2014. 3, 4, 6, 7
- [36] Shikun Liu, Shuaifeng Zhi, Edward Johns, and Andrew J. Davison. Bootstrapping semantic segmentation with regional contrast. *arXiv preprint arXiv:2104.04465*, 2021. 4, 6, 7
- [37] Ze Liu, Yutong Lin, Yue Cao, Han Hu, Yixuan Wei, Zheng Zhang, Stephen Lin, and Baining Guo. Swin transformer: Hierarchical vision transformer using shifted windows. *CVPR*, 2021. 3
- [38] Anthony Martin. Recycling image classification. [EB/OL]. <http://web.cecs.pdx.edu/~singh/rcyc-web/index.html>/ Accessed May 22, 2021. 1, 3
- [39] Francisco Massa and Ross Girshick. maskrcnn-benchmark: Fast, modular reference implementation of Instance Segmentation and Object Detection algorithms in PyTorch. <https://github.com/facebookresearch/maskrcnn-benchmark>, 2018. Accessed: [Insert date here]. 3, 6
- [40] Robert Mendel, Luis Antonio de Souza, David Rauber, João Paulo Papa, and Christoph Palm. Semi-supervised segmentation based on error-correcting supervision. In *ECCV*, 2020. 4
- [41] Shervin Minaee, Yuri Y Boykov, Fatih Porikli, Antonio J Plaza, Nasser Kehtarnavaz, and Demetri Terzopoulos. Image segmentation using deep learning: A survey. *IEEE Trans. on PAMI*, 2021. 3
- [42] Sudhanshu Mittal, Maxim Tatarchenko, and Thomas Brox. Semi-supervised semantic segmentation with high-and low-level consistency. *IEEE Trans. on PAMI*, 2019. 4
- [43] B. E. Moore and J. J. Corso. Fiftyone. *GitHub. Note: https://github.com/voxel51/fiftyone*, 2020. 6
- [44] Roozbeh Mottaghi, Xianjie Chen, Xiaobai Liu, Nam-Gyu Cho, Seong-Whan Lee, Sanja Fidler, Raquel Urtasun, and Alan Yuille. The role of context for object detection and semantic segmentation in the wild. In *CVPR*, 2014. 3
- [45] Yassine Ouali, Celine Hudelot, and Myriam Tami. Semi-supervised semantic segmentation with cross-consistency training. In *The IEEE/CVF Conference on Computer Vision and Pattern Recognition (CVPR)*, June 2020. 4, 6, 7
- [46] Deepak Pathak, Philipp Krahenbuhl, and Trevor Darrell. Constrained convolutional neural networks for weakly supervised segmentation. In *ICCV*, 2015. 4
- [47] Vitali Petsiuk, Abir Das, and Kate Saenko. Rise: Randomized input sampling for explanation of black-box models. *arXiv preprint arXiv:1806.07421*, 2018. 6
- [48] Pedro F Proença and Pedro Simões. Taco: Trash annotations in context for litter detection. *arXiv preprint arXiv:2003.06975*, 2020. 1, 2, 3, 6
- [49] AMP Robotics. <https://www.amprobotics.com/>. Accessed: 2020-05-30. 1
- [50] Zen Robotics. <https://zenrobotics.com/>. Accessed: 2020-05-30. 1
- [51] Boris Sekachev, Nikita Manovich, Maxim Zhiltsov, Andrey Zhavoronkov, Dmitry Kalinin, Ben Hoff, TOSmanov, Dmitry Kruchinin, Artyom Zankevich, DmitriySidnev, Maksim Markelov, Johannes222, Mathis Chenuet, a andre, telenachos, Aleksandr Melnikov, Jijoong Kim, Liron Ilouz, Nikita Glazov, Priya4607, Rush Tehrani, Seungwon Jeong, Vladimir Skubriev, Sebastian Yonekura, vugia truong, zliang7, lizhming, and Tritin Truong. opencv/cvat: v1.1.0, Aug. 2020. 5
- [52] Hoo-Chang Shin, Holger R Roth, Mingchen Gao, Le Lu, Ziyue Xu, Isabella Nogues, Jianhua Yao, Daniel Mollura, and Ronald M Summers. Deep convolutional neural networks for computer-aided detection: Cnn architectures, dataset characteristics and transfer learning. *IEEE transactions on medical imaging*, 35(5):1285–1298, 2016. 7
- [53] Nathan Silberman, Derek Hoiem, Pushmeet Kohli, and Rob Fergus. Indoor segmentation and support inference from rgb-d images. In *ECCV*, 2012. 3
- [54] Joao Sousa, Ana Rebelo, and Jaime S Cardoso. Automation of waste sorting with deep learning. In *2019 XV Workshop de Visão Computacional (WVC)*, pages 43–48. IEEE, 2019. 1, 2, 3
- [55] Xin Tao, Hongyun Gao, Xiaoyong Shen, Jue Wang, and Ji-aya Jia. Scale-recurrent network for deep image deblurring. In *IEEE Conference on Computer Vision and Pattern Recognition (CVPR)*, 2018. 5
- [56] Yude Wang, Jie Zhang, Meina Kan, Shiguang Shan, and Xilin Chen. Self-supervised equivariant attention mechanism for weakly supervised semantic segmentation. In *CVPR*, 2020. 4
- [57] Waste-Robotics. <https://wasterobotic.com/>. Accessed: 2020-05-30. 1
- [58] Yuxin Wu, Alexander Kirillov, Francisco Massa, Wan-Yen Lo, and Ross Girshick. Detectron2. <https://github.com/facebookresearch/detectron2>, 2019. 7, 12
- [59] Mengde Xu, Zheng Zhang, Han Hu, Jianfeng Wang, Lijuan Wang, Fangyun Wei, Xiang Bai, and Zicheng Liu. End-to-end semi-supervised object detection with soft teacher. *arXiv preprint arXiv:2106.09018*, 2021. 7
- [60] Mindy Yang and Gary Thung. Classification of trash for recyclability status. *CS229 Project Report*, 2016, 2016. 1, 3

- [61] Fisher Yu, Haofeng Chen, Xin Wang, Wenqi Xian, Yingying Chen, Fangchen Liu, Vashisht Madhavan, and Trevor Darrell. Bdd100k: A diverse driving dataset for heterogeneous multitask learning. In *CVPR*, 2020. 3
- [62] Yuhui Yuan, Xilin Chen, and Jingdong Wang. Object-contextual representations for semantic segmentation. *ECCV*, 2020. 3
- [63] Hengshuang Zhao, Jianping Shi, Xiaojuan Qi, Xiaogang Wang, and Jiaya Jia. Pyramid scene parsing network. In *CVPR*, 2017. 3
- [64] Bolei Zhou, Aditya Khosla, Agata Lapedriza, Aude Oliva, and Antonio Torralba. Learning deep features for discriminative localization. In *CVPR*, 2016. 4
- [65] Bolei Zhou, Hang Zhao, Xavier Puig, Sanja Fidler, Adela Barriuso, and Antonio Torralba. Scene parsing through ade20k dataset. In *CVPR*, 2017. 3

7. Appendix

7.1. Detection Experiments

In this section, we provide detailed class-wise results of object detection experiments using Mask R-CNN. Please see Table 4 for detailed results of the experiments with Mask R-CNN pretrained with COCO and TACO datasets, and the visualization of the Mask-RCNN predictions can be found on Figure 8.

Implementation details For Mask R-CNN and Trident-Net experiments, we used the default implementation and hyperparameters from the Detectron V2 [58] library. For the RetinaNet experiments, we used the open-source implementation and the default hyperparameters provided here: <https://github.com/yhenon/pytorch-retinanet>. We provide the exact code in the supplementary files.

	COCO		TACO	
	Validation	Test	Validation	Test
<i>Cardboard</i>	29.85	35.05	30.50	36.22
<i>Soft Plastic</i>	22.09	26.29	22.96	28.28
<i>Rigid Plastic</i>	15.70	14.57	16.58	16.24
<i>Metal</i>	1.64	11.97	5.20	16.53
<i>Total</i>	17.32	21.97	18.81	24.32

Table 4. Class-wise average precision results of a COCO-pretrained (**left**) and TACO-pretrained (**right**) Mask R-CNN on our ZeroWaste-*f* dataset.

7.2. Segmentation Experiments

In this section, we provide detailed class-wise results, confusion matrices, and visualizations of our segmentation experiments. Table 5 shows the segmentation results of DeepLabv3+ [14] (trained on ZeroWaste-*f*) for each class in ZeroWaste dataset. Visual predictions of DeepLabv3+, ReCo, and Puzzle-Cam [27], all trained on ZeroWasteAug, can be found in Figures 9, 10, and 11 respectively.

Implementation details For all semantic segmentation experiments, we used the default hyperparameters for all methods. We used the Detectron V2 [58] implementation for the DeepLabv3+ experiments, as well as the official implementation of ReCO (<https://github.com/lorenmt/reco>), CCT (<https://github.com/yassouali/CCT>), PuzzleCAM (<https://github.com/OFRIN/PuzzleCAM/>) and EPS (<https://github.com/neo85824/epsnet>).

7.3. Additional Data Examples

In this section, we provide further examples of frames from our ZeroWaste-*f* and ZeroWasteAug datasets. The example of a frame from ZeroWaste before and after processing as described in Section 3 can be found in Figure 12. Examples of fully annotated ZeroWaste-*f* frames can be found in Figures 13 and 14. Further, examples of augmented frames of ZeroWasteAug can be found in Figure 15.

7.4. Annotation Costs and Statistics

The total annotation cost per frame is 1.21\$, including 0.6\$ for annotation and 0.62\$ for expert review.

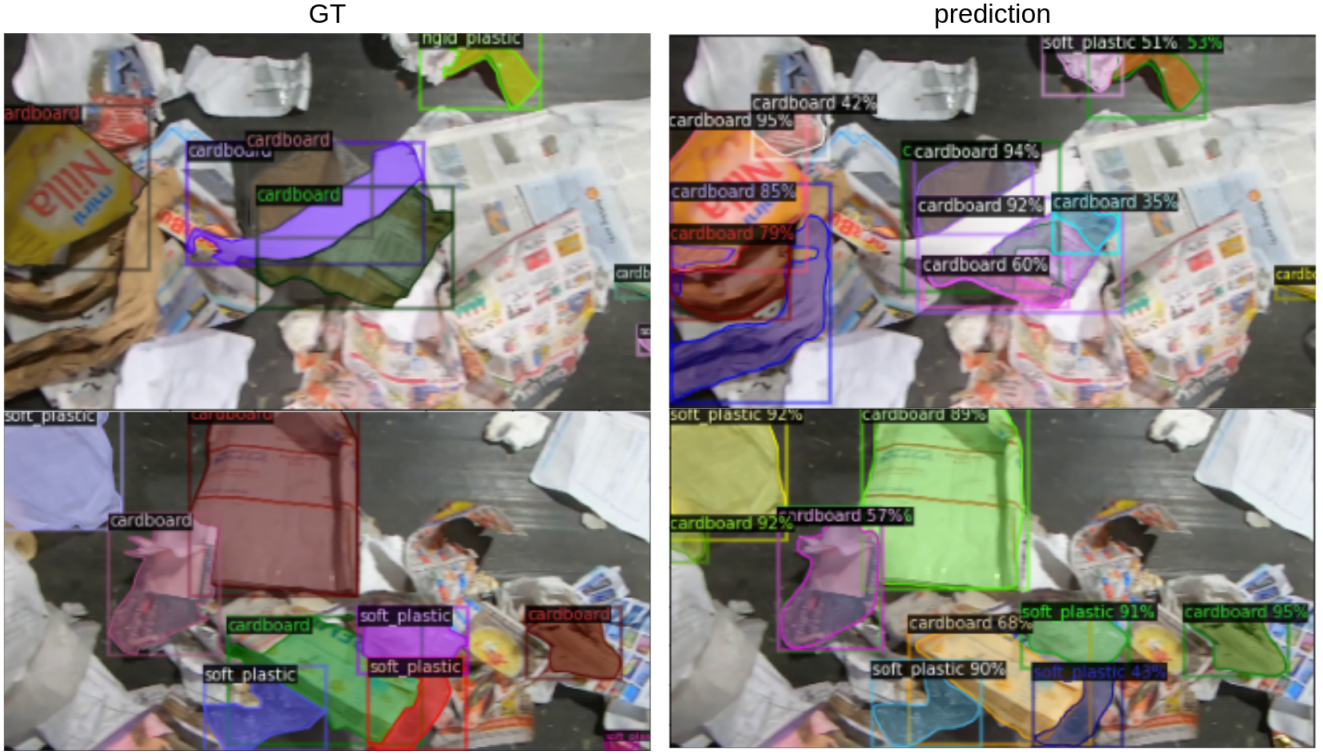


Figure 8. Examples of predictions of Mask-RCNN trained on *ZeroWaste-f*.

	Train			Validation			Test		
	IoU	Precision	Pix. Acc.	IoU	Precision	Pix. Acc.	IoU	Precision	Pix. Acc.
<i>Background</i>	94.82	96.31	98.40	90.41	92.81	97.22	91.02	93.71	96.95
<i>Cardboard</i>	69.51	89.21	75.86	51.38	79.96	58.98	54.47	77.95	64.40
<i>Soft plastic</i>	78.99	91.09	85.61	61.86	77.34	75.56	63.18	80.99	74.17
<i>Rigid plastic</i>	65.46	76.21	82.27	27.58	59.33	34.01	24.82	54.95	31.16
<i>Metal</i>	76.23	86.78	86.98	3.41	33.19	3.67	27.14	70.54	30.61
mean	77.01	87.96	85.64	46.93	83.35	53.88	52.13	75.63	59.46

Table 5. Experimental results of DeepLabv3+ [14] on our *ZeroWaste-f* dataset.

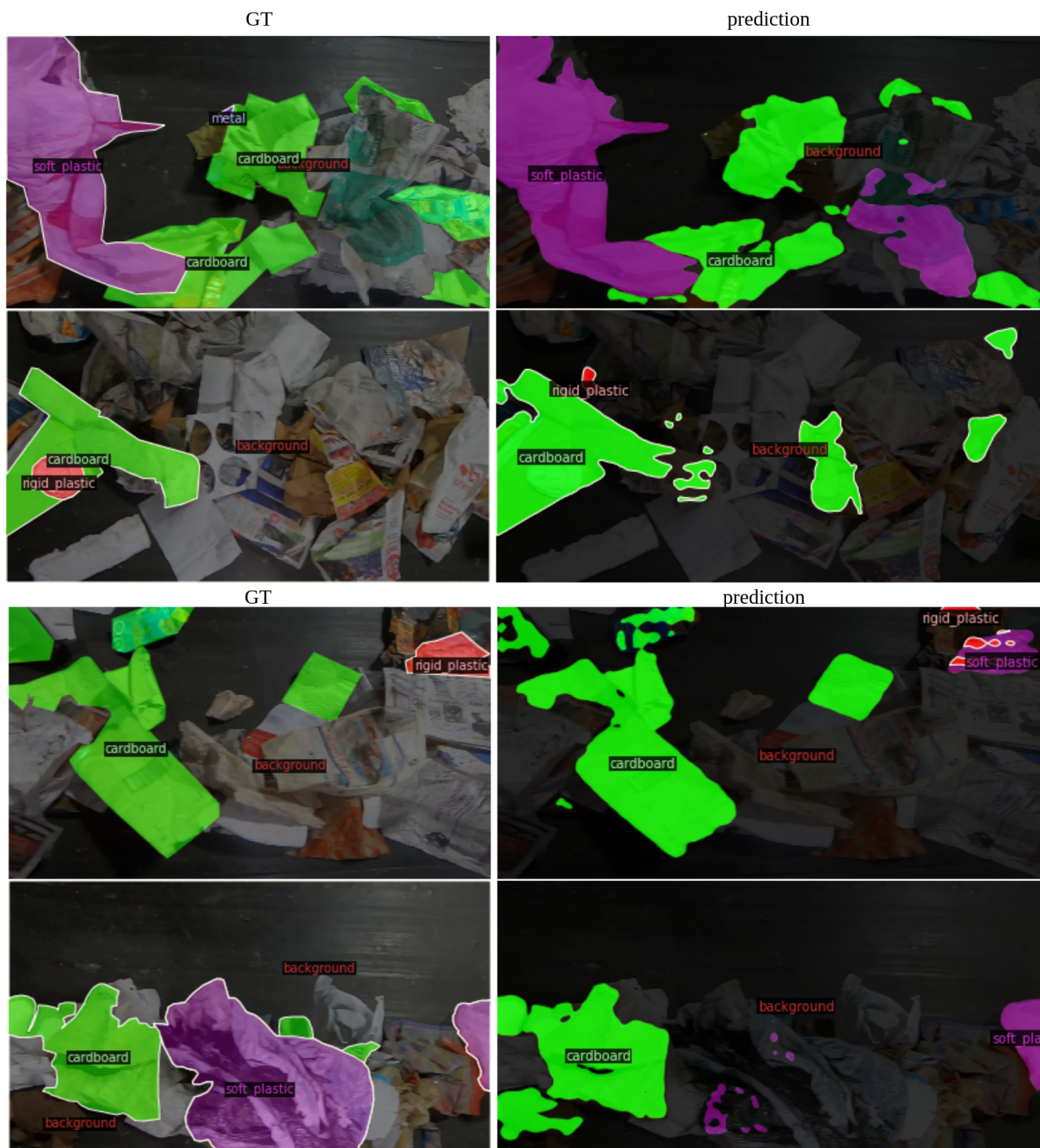


Figure 9. Examples of predictions of the fully-supervised DeepLabv3+ method trained on ZeroWaste- f .

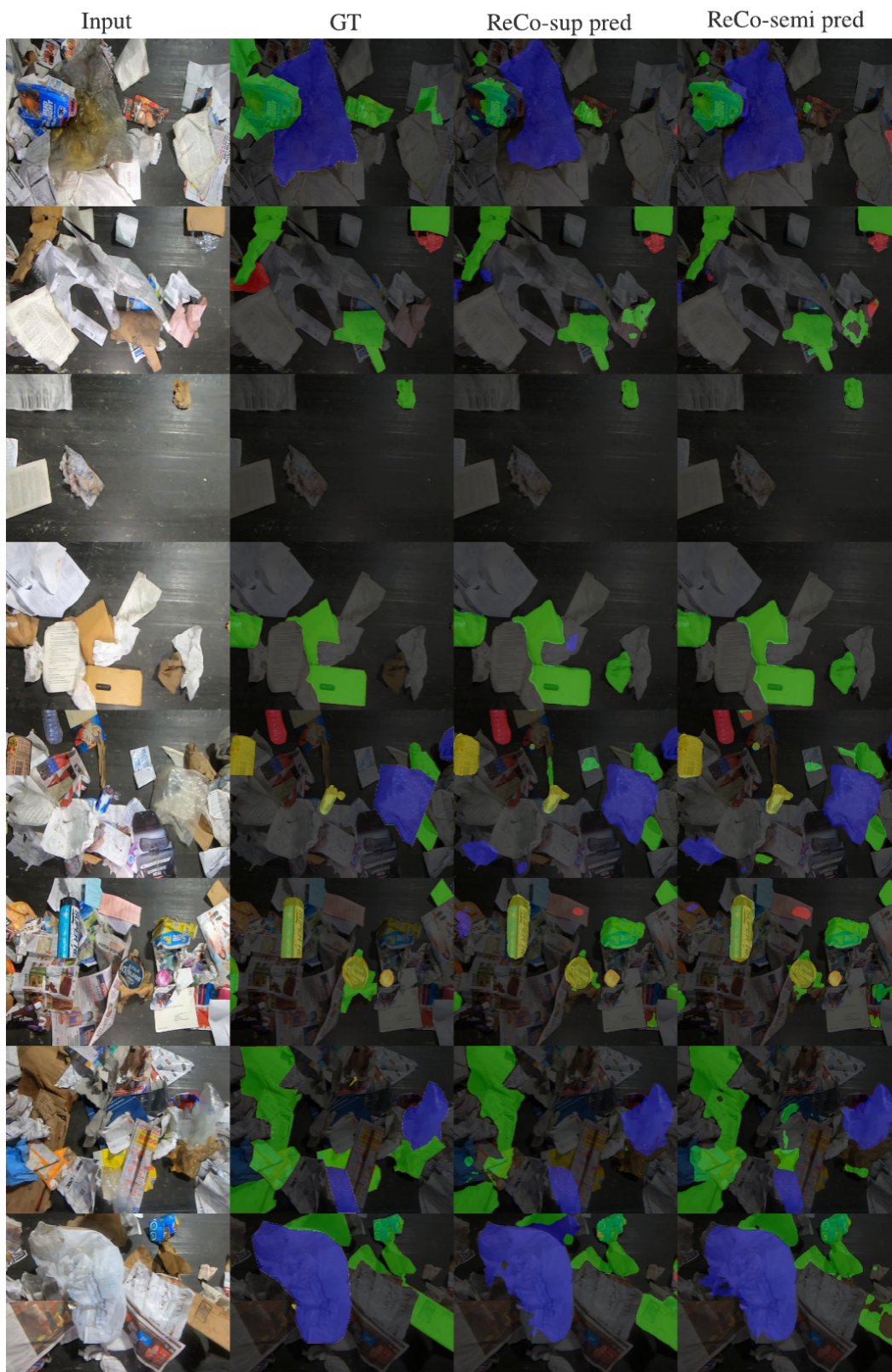


Figure 10. Examples of predictions of the supervised and semi-supervised versions of the ReCo method on the images from the validation set.



Figure 11. Examples of predictions of the weakly-supervised Puzzle-Cam trained on $\text{ZeroWaste-}w$ (before/after image-level labels).



Figure 12. **Left:** sample video frame from ZeroWaste *before* collection of target objects to be removed from the conveyor belt. **Right:** the same video frame processed as described in section 3: fisheye effect removed, frame rotated to make the conveyor belt parallel to the image border, regions outside conveyor belt cropped out, motion blur removed.



Figure 13. Examples of images (**left**) and the corresponding polygon annotation (**right**) of the proposed ZeroWaste dataset.



Figure 14. Examples of images (**left**) and the corresponding polygon annotation (**right**) of the proposed ZeroWaste dataset.



Figure 15. Examples of images from *ZeroWasteAug*. Red circles show examples of metal and rigid plastic augmented objects cropped out from TACO.

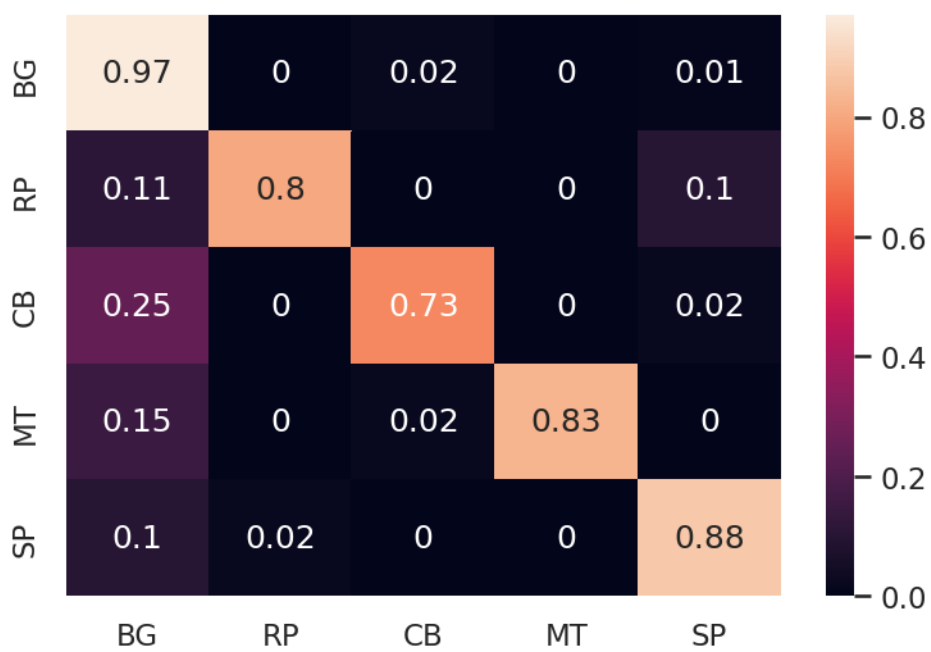


Figure 16. Confusion matrix of corresponding to average agreement across annotators over 20 frames *before* the expert review.